First-principles local-orbital calculation of the structural and electronic properties of ordered and random alloys of GaN and AlN

1999 J. Phys.: Condens. Matter 11 2351

(http://iopscience.iop.org/0953-8984/11/11/007)

J. Phys.: Condens. Matter **11** (1999) 2351–2361. Printed in the UK PII: S0953-8984(99)96440-8

First-principles local-orbital calculation of the structural and electronic properties of ordered and random alloys of GaN and AlN

Jürgen Fritsch, Otto F Sankey, Kevin E Schmidt and John B Page
Department of Physics and Astronomy, Arizona State University, Tempe, AZ 85287-1504, USA

Received 3 August 1998, in final form 13 January 1999

Abstract. We have investigated the lattice parameters, bond lengths, and band-gap energies of ordered and random $Al_xGa_{1-x}N$ alloys of wurtzite-phase AlN and GaN, using density-functional local-orbital theory based on the local-density approximation and the pseudopotential method. The lattice constants a and c are found to change nearly linearly with x for all structures. However, the Ga–N and Al–N bond lengths exhibit significantly smaller variations, which is in agreement with the data from recent x-ray absorption fine-structure measurements. The alloys are direct-gap semiconductors for all Al fractions x. The alloy structures investigated exhibit a small downward bowing of the band-gap energy. The bowing is substantially reduced by optimizing the lattice parameters. For ordered alloys, the band-gap energies are found to show a nearly linear variation with the Al fraction.

1. Introduction

In semiconductor technology, group-III nitrides are promising materials which are attracting increasing attention due to the steady improvement of the quality and homogeneity of their films. Alloys of AlN and GaN are of particular importance. Because of the large difference between the electronic band-gap energies of the two materials, optoelectronic devices can be designed that cover a wide spectral range from the visible to the ultraviolet. Typically, thin group-III nitride films are grown in the more stable wurtzite phase, using hexagonal surfaces of sapphire and 6H-SiC as substrates for molecular beam epitaxy (MBE) or metal–organic chemical vapour deposition (MOCVD).

Numerous experiments have been performed to explore the structural and electronic properties of thin wurtzite-phase GaN and AlN films and their alloys. The lattice constants of $Al_xGa_{1-x}N$ are found to vary nearly linearly with the Al fraction x [1–5]. The individual Ga–N and Al–N bond lengths, however, change only to a small extent with composition and therefore remain close to the nearest-neighbour distances of the pure materials. This behaviour, which was revealed for $Al_xGa_{1-x}N$ by recent x-ray absorption fine-structure (EXAFS) measurements [6], is common for III–V alloys such as $Ga_xIn_{1-x}As$ [7] and $Ga_xIn_{1-x}P$ [8]. As pointed out in reference [8], the remaining slight variations of the bond lengths are smaller for ordered alloys than for their random counterparts.

Ordering may also influence the electronic band-gap energy. On the basis of linear augmented-plane-wave calculations, an ordering-induced band-gap narrowing was found for many III–V pseudobinary alloys [9]. For thin wurtzite-phase $Al_xGa_{1-x}N$ films, optical absorption measurements [1, 3, 4] revealed a nearly linear variation of the band-gap energy

0953-8984/99/112351+11$19.50

with the alloy composition. Bowing was found to be negligible in reference [1], while small deviations from a linear behaviour were found in references [3] and [4].

Up to now, only a few theoretical studies have focused on determining the structural and electronic properties of $Al_xGa_{1-x}N$ alloys [10–15]. Most of these calculations were carried out for alloys with zinc-blende structure. Some of them have relaxed the unit-cell volume [10–12] and the internal degrees of freedom [10, 11]. In contrast, the atomic positions and the lattice constants were chosen according to the virtual-crystal approximation (VCA) in references [13] and [14]. To model random alloys, a cluster expansion method was used in references [11] and [12], while the investigations of reference [10] used special quasi-random structures. Supercells with eight Ga and eight Al atoms randomly placed at the cation sites were used in the studies of reference [15]. In reference [13], alloys with zinc-blende and wurtzite symmetry were investigated. The computations of references [10–15] confirm that the lattice constants vary nearly linearly with the alloy composition and yield a small downward bowing of the electronic band-gap energy. As discussed in reference [16] for GaPN and GaAsN alloys, it is important to account for the influence of ordering versus disordering, as well as effects related to bond-length relaxations and non-linearities of the lattice constants. This has not yet been analysed in full detail for the $Al_xGa_{1-x}N$ alloys.

In this paper, we present the results of a comprehensive theoretical study of the atomic structure and electronic properties of wurtzite-phase $Al_xGa_{1-x}N$ alloys. We perform density-functional local-orbital calculations for ordered and random alloys, covering the complete range from zero to one for the Al fraction x. The lattice parameters and the individual Al–N and Ga–N bond lengths are determined by minimizing the total energy with respect to the dimensions of the unit cell, including a relaxation of all internal degrees of freedom. Vegard's law is found to be valid for all systems studied, with only small deviations. The Al–N and Ga–N bond lengths differ only slightly from the respective values in the pure bulk materials; the smallest changes are realized in ordered structures. Our results are in good agreement with the recent EXAFS experiments. We compare the electronic band structure of random alloys and ordered structures. The direct band gap shows a small downward bowing for random alloys and for incompletely optimized ordered structures. Ordered alloys for which all degrees of freedom are relaxed, including the dimensions of the unit cell, give a nearly linear variation of the band-gap energy.

2. Theoretical method

Our calculations are carried out by means of a multicentre local-orbital formalism [17–20], which is based on density-functional theory in the local-density approximation [21–24] and the use of norm-conserving pseudopotentials [25]. The electronic wave functions are represented by a superposition of pseudo-atomic orbitals (PAO) comprising the valence electron s and p orbitals for N, Al, and Ga. The Ga 3d state is not included in our minimal-basis local-orbital formalism. The valence charge density is approximated by

$$n_{in}(\boldsymbol{r}) = \sum_i n_i |\phi_i(\boldsymbol{r} - \boldsymbol{R}_i)|^2 \tag{1}$$

which is used as the input charge density for the Harris functional approach [26] applied to compute the total energy [17]. The occupation numbers n_i of the PAOs $\phi_i(\boldsymbol{r} - \boldsymbol{R}_i)$ are determined in a self-consistent fashion as described in reference [19].

The PAOs are constructed self-consistently under the boundary condition that the PAOs vanish beyond a specified cut-off radius r_c. Confined atomic orbitals significantly improve the accuracy of the Harris functional, since they simulate the contraction of the atomic charge

Table 1. The lattice constants a and c, internal parameter u, bulk modulus B_0, and band-gap energy E_{gap} of wurtzite-phase GaN and AlN.

	Wurtzite GaN		Wurtzite AlN	
	Present Work	Experiment	Present Work	Experiment
a (Å)	3.115	3.190[a]	3.031	3.110[a]
c (Å)	5.076	5.189[a]	4.896	4.980[a]
c/a	1.629	1.627[a]	1.615	1.601[a]
u	0.377	0.377[a]	0.381	0.382[a]
B_0 (Mbar)	1.57	—	2.43	2.02[b]
E_{gap} (eV)	4.83	3.39[c]	7.61	6.20[c]

[a] Experimental data from reference [28].
[b] Experimental data from reference [29].
[c] Experimental data from reference [2].

density observed in solid-state systems [27]. We use $r_c = 5.4$ (atomic units) for gallium, $r_c = 5.4$ for aluminium, and $r_c = 3.8$ for nitrogen, to compute all interaction terms and overlap integrals. The only deviation from using these values is that we compute the Coulomb integrals in the electron double-counting correction U_{ee} (see reference [17]) using less confined PAOs for gallium ($r_c^{\text{Coul}} = 5.75$), aluminium ($r_c^{\text{Coul}} = 5.9$), and nitrogen ($r_c^{\text{Coul}} = 3.95$). Table 1 summarizes the lattice parameters and bulk moduli obtained with our choice of radii and compares the results with experimental data. Our calculations give the same underestimation of about 2% for the lattice parameters a and c of GaN and AlN. The computed electronic band-gap energies for GaN and AlN are 4.83 and 7.61 eV. These values are about 1.4 eV larger than the band-gap energies 3.39 and 6.20 eV measured for the two materials [2]. The overestimation results from the small number of orbitals used to represent the electronic wave functions in our calculations [30].

As demonstrated by computations carried out within the full-potential linear muffin-tin orbitals method or the plane-wave pseudopotential approach [31, 32], the Ga 3d electrons should be included in order to obtain correct results for the electronic properties and the bonding structure. The studies of reference [31] show that the N 2s-derived valence bands hybridize substantially with the Ga 3d bands. However, the top valence band, which is dominated by the N 2p states, is essentially not influenced by the Ga 3d electrons. Therefore, the dispersion of the highest valence band and the lowest conduction band can be computed with our method in accord with the results of the previous investigations, although the Ga 3d electrons are not treated explicitly as valence states. We have checked this by comparing the electronic dispersion computed for zinc-blende phase GaN with the findings of reference [31]. The agreement also follows from the fact that the lattice parameters calculated by us for GaN and AlN are close to the respective experimental data. This was achieved in our method by determining the Coulomb integrals in the electron double-counting correction with slightly less confined PAOs, which basically mimics an increase of interatomic repulsion as caused, for instance, by the presence of semi-core states.

3. Alloy structures investigated

Our computations for ordered and random alloys are carried out using a $2 \times 2 \times 2$ supercell which has twice the size of the primitive wurtzite unit cell in both directions of the basal plane and along the c-axis. Although the size of the supercell is relatively small, our results

computed for random alloys appear to be sufficiently converged, in agreement with the findings of reference [15]. Brillouin zone integrals are approximated by sampling at nine special $\boldsymbol{k}$-points which correspond to a $6 \times 6 \times 4$ mesh. We only use time-reversal symmetry to reduce the number of points in the $\boldsymbol{k}$-point mesh. With this, we are able to relax all atomic degrees of freedom without symmetry constraints. The 16 cation lattice sites per unit cell allow us to investigate $Al_xGa_{1-x}N$ alloys with the Al fraction x being an integer multiple of 1/16. X-ray measurements [1–5] have found that Vegard's law holds with only small deviations. Hence the dimensions of the supercell may be chosen as the average values

$$a_{\mathrm{VCA}} = 2[x a_{\mathrm{AlN}} + (1 - x) a_{\mathrm{GaN}}] \tag{2}$$

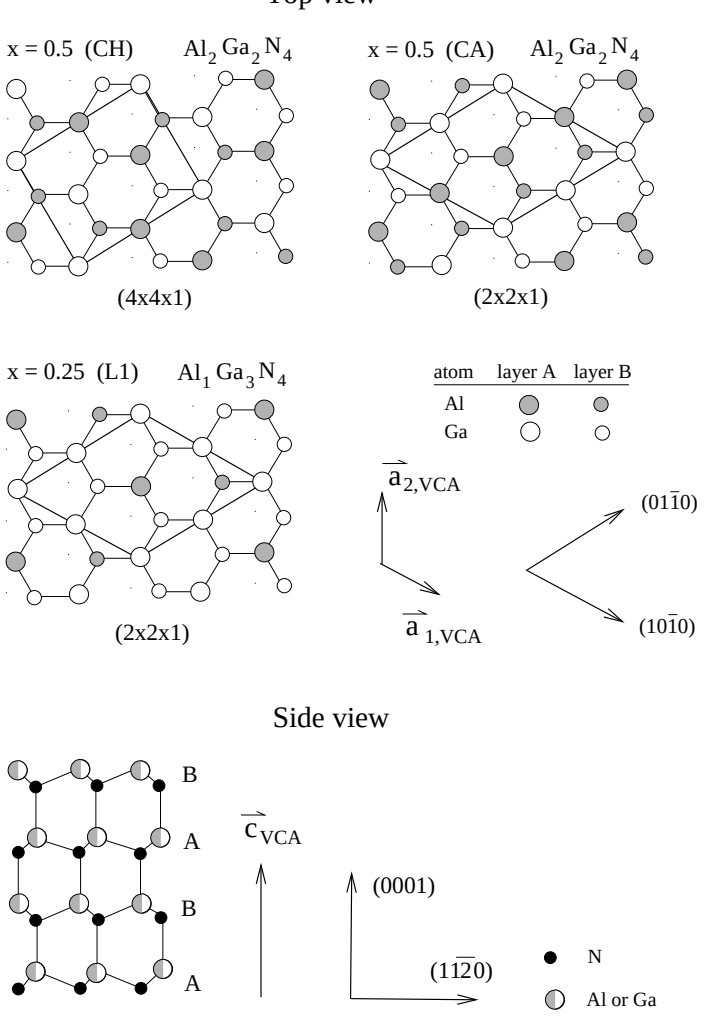

Figure 1. Top and side views of the ordered $Al_xGa_{1-x}N$ alloys studied for $x = 0.25, 0.5$, and 0.75. The superstructure index $(n_1 \times n_2 \times n_3)$ for each configuration is given with respect to the primitive translations $\boldsymbol{a}_{1,\mathrm{VCA}}$, $\boldsymbol{a}_{2,\mathrm{VCA}}$, and $\boldsymbol{c}_{\mathrm{VCA}}$ of the VCA crystal. The solid lines in the top view illustrate the unit cells used in our calculations. To obtain the ordered structure for $x = 0.75$, all Ga and Al atoms of the L1 configuration are exchanged with their counterparts.

and

$$c_{\mathrm{VCA}} = 2[x c_{\mathrm{AlN}} + (1-x) c_{\mathrm{GaN}}]. \tag{3}$$

All atoms in the supercell are relaxed with respect to the Hellmann–Feynman forces. To estimate the deviations from Vegard's law, optimal values for a and c that minimize the total energy are determined for some of the alloy structures.

To describe random alloys for a given fraction $x = n/16$, we occupy the 16 cation sublattice positions in the supercell arbitrarily with n Al atoms and $16 - n$ Ga atoms. Out of the $\binom{16}{n}$ possible configurations, we randomly choose three arrangements. To check possible effects caused by the limited randomness and the limited size of the $2 \times 2 \times 2$ cell, additional random configurations and larger supercells would have to be considered. Already for a $2 \times 2 \times 2$ supercell, however, quantities such as the average of the nearest-neighbour bond lengths show only a very small dependence on the particular random configuration selected for the alloy. This indicates that the randomness of disordered alloys and their bonding properties can be described well enough by the chosen random configurations and the size of the supercell. In a calculation of the electronic band-gap energy, a similar conclusion was found in reference [15].

In addition to random alloys, we have also considered ordered superstructures. Figure 1 illustrates the atomic structure of the three ordered alloys that we consider for $x = 0.25$, $x = 0.5$, and $x = 0.75$. The top view of one pair of cation layers A and B already gives a complete representation of the atomic structure of the ordered alloys investigated here. For the Al fraction $x = 0.5$, we consider the structures CH and CA which are pictured in the upper part of figure 1. The structure L1 studied for $x = 0.25$ can be obtained from the configuration CA by replacing every other Al atom by one Ga atom. For $x = 0.75$ we use the L2 geometry, which is derived from L1 by exchanging all group-III atoms with their respective counterparts. The structures CA, CH, L1, and L2 are the wurtzite-phase analogues of the respective zinc-blende-phase geometries CA, CH, L1, and L2 illustrated in figure 2 of reference [33].

4. Results

The lattice constants of a III–V pseudobinary alloy are usually close to the composition average of the lattice parameters of the end-point materials which form the alloy. As can be seen from table 1, our calculated lattice constants a and c of AlN are smaller than those of GaN by 2.7 and 3.5%. X-ray measurements give differences of 2.5 and 4.0% [28]. Numerous experiments show that the lattice parameters a and c of the wurtzite-phase $Al_xGa_{1-x}N$ alloys essentially obey Vegard's law with only small deviations [1–3]. To estimate the magnitude of the deviations, we optimize the lattice parameters for some of the alloy structures described in section 3. Optimal values for a and c are found by computing total energies on a 4×4 grid of 16 points which is given by all combinations of a/a_{VCA} and c/c_{VCA} chosen from the values

$$a/a_{\mathrm{VCA}}, c/c_{\mathrm{VCA}} \in \{0.985, 0.995, 1.005, 1.015\}. \tag{4}$$

For each given pair (a, c) on the grid, the internal degrees of freedom in the unit cell are relaxed with respect to the Hellmann–Feynman forces. By fitting the 16 total-energy values to a cubic equation in the cell volume V and the ratio c/a, in analogy to reference [34], we find the equilibrium values for the lattice parameters a and c. Figure 2 illustrates the total energies computed for the ordered alloy structures CH and CA. The energy of the CH configuration is minimal for $a = 0.996\, a_{\mathrm{VCA}}$ and $c = 0.999\, c_{\mathrm{VCA}}$, while the optimal lattice parameters for the CA structure are $a = 0.998\, a_{\mathrm{VCA}}$ and $c = 0.999\, c_{\mathrm{VCA}}$. Hence, the lattice parameters essentially follow Vegard's law. The same result holds for the structures L1 and L2, as well as for the one arbitrarily selected random alloy configuration which we have chosen for the lattice

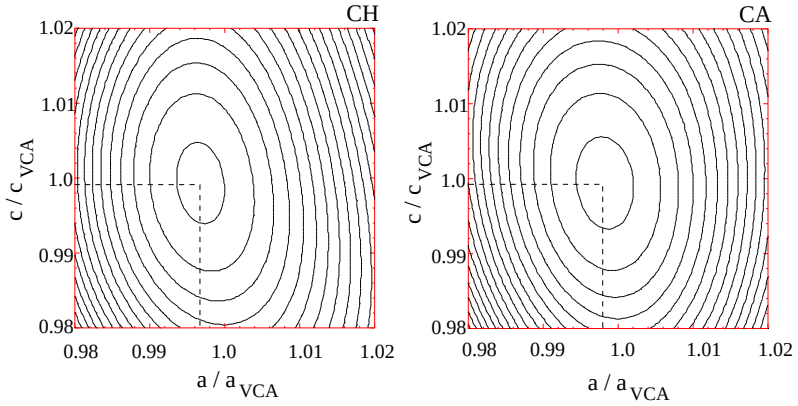

Figure 2. Total energies of the ordered alloy structures CH (left) and CA (right) as functions of the lattice parameters a and c. The contour step is 1.45 meV for the CH structure and 1.5 meV for the CA configuration.

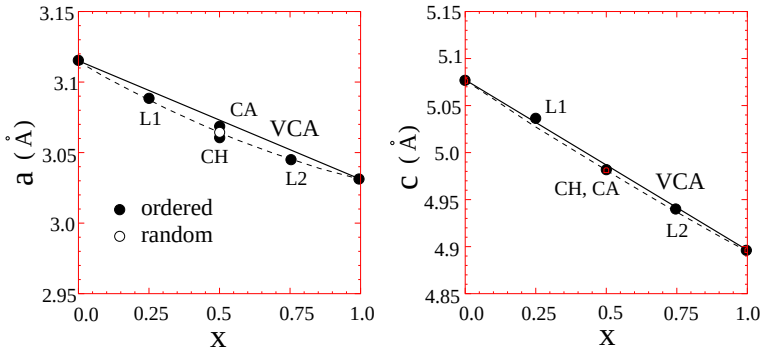

Figure 3. Optimal lattice constants a and c computed for one random alloy structure with $x = 0.5$, as well as for the ordered structures CH, CA, L1, and L2. The solid lines correspond to the virtual-crystal approximation (VCA), while the broken curves indicate the slight bowing.

parameter optimization. A comparison of our results for these structures is given in figure 3. In each case, the lattice parameters leading to the lowest total energy are close to the respective VCA values. In particular, the hexagonal-axis lattice constant c varies essentially linearly with the alloy composition, in agreement with the x-ray measurements of references [1–3]. The in-plane lattice constant a shows a small downward bowing. As discussed in more detail below, the average bond lengths computed for various random sets of a given Al fraction are essentially independent on the particular choice of the respective random structure. This indicates that the deviation from Vegard's law observed for the arbitrarily chosen disordered structure can be expected to be similar for all random alloy configurations.

The change of the lattice constants with the Al fraction x originates in small variations of the individual Ga–N and Al–N bond lengths and, to a significant degree, in bond-angle distortions. To determine the extent to which the nearest-neighbour distances decrease as a function of the composition index x, we perform a large number of calculations for ordered and random alloys covering the entire range $0 \leqslant x \leqslant 1$. In this part of our investigation, the dimensions of the unit cells are chosen according to Vegard's law for all alloy structures. The average of the Ga–N and Al–N nearest-neighbour distances is determined by sampling over

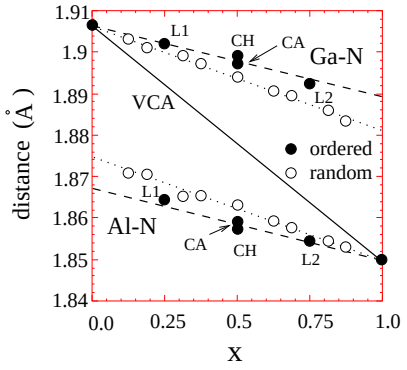

Figure 4. Variations of the averaged Ga–N and Al–N bond lengths in $Al_xGa_{1-x}N$ as functions of the alloy composition. Open circles illustrate the results computed for random alloys, while filled circles represent our results for ordered alloys. The structures CH, CA, L1, and L2 are pictured in figure 1.

all respective bonds in the unit cell after relaxing the atoms into their zero-force positions. To describe random alloys, three arbitrarily selected configurations are used for each given Al fraction x. The average bond lengths computed for the three individual random arrangements differ by less than 0.003 Å and therefore nearly coincide with their mean value which is used to represent the respective quantity of the random alloy. As can be seen from figure 4, the Ga–N and Al–N bond lengths vary by a considerably smaller amount than predicted by the VCA. As a result, the nearest-neighbour Ga–N distances are substantially larger than the Al–N bond lengths in $Al_xGa_{1-x}N$, for each Al fraction. For disordered alloys, the Ga–N and Al–N bond lengths exhibit essentially a linear variation with x. The deviations from the linear behaviour are also negligible for each individual random configuration selected in our computations. Effects stemming from the restriction to the small size of our supercell and the limited degree of randomness are not evident.

The two dissimilar bond lengths in the alloys can be accommodated by bond-angle distortions, related to the fact that bond-bending force constants are usually smaller than bond-stretching force constants. Hence, the strain energy in the alloys can be minimized by reducing the variation of each individual bond length at the expense of larger bond-angle deformations. In contrast with random configurations, changes of the bond angles occur in a coherent fashion in ordered structures. Therefore, the nearest-neighbour bond lengths vary by a smaller degree with respect to the corresponding values of the pure end-point materials in ordered alloys than in random alloys. This is consistent with the results of computations performed for $Ga_xIn_{1-x}P$ [8].

Our data for the ordered alloys give the best agreement with the findings of recent EXAFS measurements [6], in which the change of the Ga–N bond lengths was resolved for $0 \leqslant x \leqslant 0.45$. By fitting the values computed for the ordered alloys to a linear equation, we obtain a slope of -0.017 Å, which is indicated by the dashed line in figure 5(b). For the experimental data, excluding the point at $x \approx 0.45$, we obtain a linear decrease with x of slope -0.015 Å, shown by the dashed line in figure 5(a). The error bars were not included in our fitting procedure. The good agreement suggests that ordering is present to some extent in the alloy films studied by EXAFS. However, no signs of the formation of ordered alloys were reported in reference [6]. Additional evidence for ordering is provided by the findings of a recent x-ray diffraction experiment in which long-range order was unambiguously detected

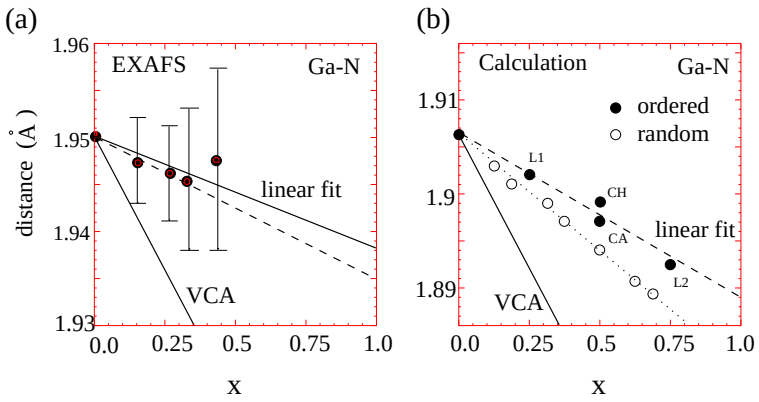

Figure 5. The variation of the Ga–N bond length in $Al_xGa_{1-x}N$ as a function of the alloy composition. (a) Experimental data from reference [6]. The solid line represents the result from a linear fit to all data points, while the Ga–N bond length determined for $x \approx 0.45$ was excluded in the fit yielding the dashed line. The slopes of the solid and dashed lines are -0.013 and -0.015 Å. (b) Average Ga–N bond lengths computed for ordered alloys (filled circles) and random alloys (open circles). Fitting the data points to a linear equation yields the slopes -0.025 and -0.017 Å, indicated by the dotted and dashed lines. The slope predicted by the VCA is -0.056 Å for both figures. The structures CH, CA, L1, and L2 are illustrated in figure 1.

for MBE-grown $Al_xGa_{1-x}N$ films [35].

In contrast with the Ga–N and Al–N bond lengths, the average of the second-neighbour cation–cation distances varies to the same extent as the lattice constants. This is clearly seen in figure 6, which compares the respective results from the EXAFS measurements with those of our computations. The large variation of the Ga–Ga, Ga–Al, and also the Al–Al distances shows that the dimensions of the cation sublattice (and of the anion sublattice) closely follow Vegard's law. In particular, the standard deviation of the individual cation–cation distances from their mean value is very small. For the ordered alloys CA and CH, the standard deviation of the Ga–Ga distances is 0.006 Å, while the respective value determined for random alloys

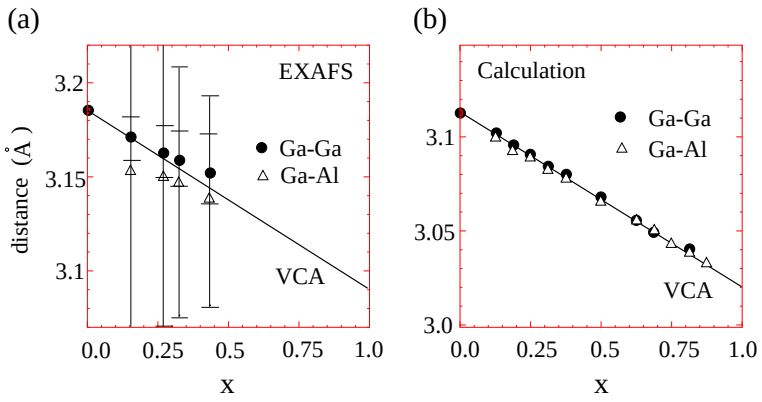

Figure 6. The variation of the averaged Ga–Ga (dots) and Ga–Al (triangles) second-neighbour distances in $Al_xGa_{1-x}N$, as a function of the alloy composition. (a) Experimental data from EXAFS [6]. The larger error bars for each x apply to the Ga–Al distances. (b) Calculated second-neighbour distances for ordered and random alloys.

with $x = 0.5$ is 0.008 Å. The standard deviation of the N–N distances in the corresponding anion sublattices is much larger. We obtain 0.035 Å for the ordered structures and 0.032 Å for the random alloys with $x = 0.5$. This means that the cation positions are close to their ideal positions in the VCA sublattice, while the nitrogen atoms in the anion sublattice exhibit large relaxations. As illustrated in figures 4 and 5, such relaxations change the individual cation–anion bond lengths only to a limited extent. The relaxations in the anion sublattice are mainly supported by bond-angle distortions.

The change of the Al–N and Ga–N bond lengths with respect to the values of the end-point materials is particularly small in ordered alloys, where bond-angle variations can be realized in a coherent fashion. This was checked by calculating the distribution of the cation–nitrogen–cation bond angles for each of the alloy structures investigated. Random alloys are characterized by a broad distribution, while in ordered alloys only a small number of characteristic bond angles occur. In the ordered alloy CA, three different Ga–N–Ga bond angles are present, namely 108.5°, 109.1°, and 110.8°. The respective values for Al–N–Al are 108.0°, 109.3°, and 111.7°. Five different angles are found in the ordered structure CH. In the structures L1 and L2, only two different angles occur for Ga–N–Ga and Al–N–Al. The number of different angles obtained for random alloys, however, is much larger. In the broad distribution of Ga–N–Ga bond angles computed at $x = 0.5$, there are two main peaks at 109.1° and 110.7°. The respective values found for the Al–N–Al bond angles are 109.4° and 111.0°.

Wurtzite-phase GaN and AlN are direct-band-gap semiconductors with measured gap energies of 3.39 and 6.20 eV, respectively [2]. Our computations yield 4.83 and 7.61 eV for GaN and AlN. Hence, the experimental data are overestimated by approximately the same amount of ∼1.4 eV for each of the two end-point materials. Because of this, we are able to reliably calculate the variation of the electronic band-gap energy as a function of the composition. We find good agreement with experimental data. Figure 7(b) summarizes our results for random and ordered alloys. By using the VCA values for the lattice parameters a and c, we obtain a small downward bowing of the band-gap energies, as illustrated by the filled and open circles. The dashed curve was determined by fitting the data points computed for

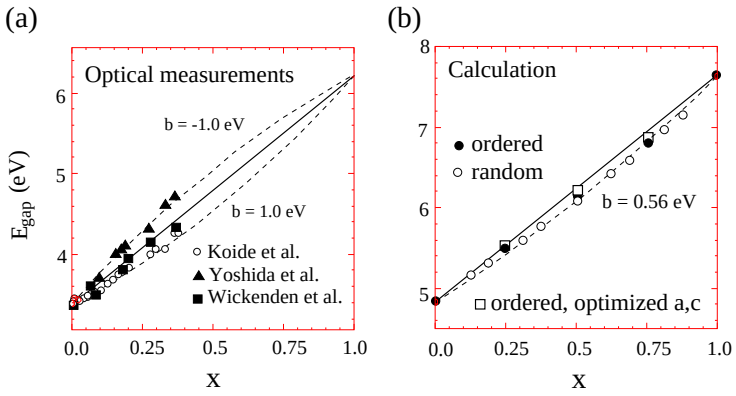

Figure 7. The electronic band-gap energy of $Al_xGa_{1-x}N$ as a function of the alloy composition. (a) Experimental results from optical measurements are taken from reference [1] (squares), reference [3] (open circles), and reference [5] (triangles). The dashed curves illustrate a bowing of ±1.0 eV. (b) Computed band-gap energies for random alloys (open circles) and ordered alloys calculated with the VCA values for the lattice constants a and c (filled circles) and the optimized values for a and c (squares). The data represented by the filled circles give a bowing of 0.56 eV, as indicated by the dashed curve.

the ordered alloys to a quadratic equation, which gave a bowing of $0.56x(1-x)$ eV. Since the optimal lattice parameters a and c are slightly smaller than those predicted by Vegard's law, the downward bowing is reduced if a and c are chosen according to figure 3. This correction leads to a nearly linear variation of the band-gap energies for the ordered alloys, as illustrated by the squares in figure 7(b). Also for random alloys, the gap energy is expected to exhibit a nearly linear variation with the Al fraction. The gap energy of the random alloy configuration chosen for the optimization of a and c is increased from 6.08 eV to 6.17 eV, reducing the bowing to about 0.2 eV.

The results from optical measurements performed for thin $Al_xGa_{1-x}N$ films are summarized in figure 7(a). While the data of Wickenden and co-workers essentially exhibit a linear variation with the Al fraction [1], a slight downward bowing was observed by Koide and co-workers [3]. This difference can be partly related to the larger increase of the non-uniformity in the alloy films, estimated in reference [3] from the larger broadening of the x-ray rocking curves. The points represented by the triangles in figure 7(a) illustrate the measured data of reference [5]. They follow a slight upward bowing resulting from the pronounced decrease of the alloy lattice parameter c reported in reference [5], which is probably related to the lattice mismatch between the substrate and the alloy film. The observation that a decrease of the lattice parameters increases the band-gap energy is consistent with our results. However, our optimization of the lattice parameters a and c yields only a slight decrease of a and c with respect to their VCA values. This increases the band-gap energy in a moderate way and hence only reduces its downward bowing, while a too-small lattice parameter such as is caused by growth on a non-matching substrate can lead to an upward bowing of the band-gap energy.

In summary, we have performed density-functional local-orbital calculations to study the structural and electronic properties of wurtzite-phase $Al_xGa_{1-x}N$ alloys. The lattice constants a and c closely follow Vegard's law. A small downward bowing occurs for a, while it is negligible for c. The variations of the individual Ga–N and Al–N bond lengths are much smaller than those of the lattice constants, due to significant bond-angle distortions. Supported by coherent bond-angle variations, the smallest bond-length changes occur in ordered alloys which give first-neighbour distances in good agreement with data from recent EXAFS experiments. Ordering and relaxation of all degrees of freedom, including the dimensions of the unit cell, also influence the electronic band-gap energy. The linear increase with x as observed by optical measurements is closely reproduced for fully optimized alloy structures, while not entirely relaxed structures exhibit a slight downward bowing. The optimization of the lattice parameters of random alloy structures also reduces the bowing.

Acknowledgments

This work was supported by the Alexander–von Humboldt foundation through a *Feodor-Lynen-Forschungsstipendium*, the National Science Foundation (Grant No DMR-9632635 and Grant No DMR-9510182), and the Office of Naval Research (N00014-95-1-0122).

References

[1] Wickenden D K, Bryden W A, Kistenmacher T J, Bythrow P F and Strohbehn K 1995 *APL Tech. Dig.* **16** 246
[2] Koide Y, Itoh H, Sawaki N, Akasaki I and Hashimoto M 1986 *J. Electrochem. Soc.* **133** 1956
[3] Koide Y, Itoh H, Khan M R H, Hiramatsu K, Sawaki N and Akasaki I 1987 *J. Appl. Phys.* **61** 4540
[4] Itoh K, Amano H, Hiramatsu K and Akasaki I 1991 *Japan. J. Appl. Phys.* **30** 1604
[5] Yoshida S, Misawa S and Gonda S 1982 *J. Appl. Phys.* **53** 6844
[6] Miyano K E, Woicik J C, Robins L H, Bouldin C E and Wickenden D K 1997 *Appl. Phys. Lett.* **70** 2108
[7] Mikkelsen J C Jr and Boyce J B 1983 *Phys. Rev.* B **28** 7130

[8] Srivastava G P, Martins J L and Zunger A 1985 *Phys. Rev.* B **31** 2561
[9] Wei S-H and Zunger A 1990 *Appl. Phys. Lett.* **56** 662
[10] Wright A F and Nelson J S 1995 *Appl. Phys. Lett.* **66** 3051
[11] Albanesi E A, Lambrecht W R L and Segall B 1993 *Phys. Rev.* B **48** 17 841
[12] Agrawal B K, Agrawal S, Yadav P S and Kumar S 1997 *J. Phys.: Condens. Matter* **9** 1763
[13] Rubio A, Corkill J L and Cohen M L 1994 *Phys. Rev.* B **49** 1952
[14] Fan W J, Li M F, Chong T C and Xia J B 1996 *J. Appl. Phys.* **79** 188
[15] van Schilfgaarde M, Sher A and Chen A-B 1997 *J. Cryst. Growth* **178** 8
[16] Bellaiche L, Wei S-H and Zunger A 1997 *Appl. Phys. Lett.* **70** 3558
[17] Sankey O F and Niklewski D J 1989 *Phys. Rev.* B **40** 3979
[18] Sankey O F, Drabold D A and Adams G B 1991 *Bull. Am. Phys. Soc.* **36** 924
[19] Demkov A A, Ortega J, Sankey O F and Grumbach M P 1995 *Phys. Rev.* B **52** 1618
[20] Ortega J, Lewis J P and Sankey O F 1994 *Phys. Rev.* B **50** 10 516
[21] Hohenberg P and Kohn W 1964 *Phys. Rev.* **136** B864
[22] Kohn W and Sham L J 1965 *Phys. Rev.* **140** A1133
[23] Ceperley D M and Alder B J 1980 *Phys. Rev. Lett.* **45** 566
[24] Perdew J P and Zunger A 1981 *Phys. Rev.* B **23** 5048
[25] Hamann D R, Schlüter M and Chiang C 1979 *Phys. Rev. Lett.* **43** 1494
[26] Harris J 1985 *Phys. Rev.* B **31** 1770
[27] Finnis M 1990 *J. Phys.: Condens. Matter* **2** 331
[28] Schulz H and Thiemann K H 1977 *Solid State Commun.* **23** 815
[29] Tsubouchi K, Sugai K and Mikoshiba N 1981 *Ultrasonics Symp. Proc.* vol 1 (New York: IEEE)
[30] Jansen R W and Sankey O F 1987 *Phys. Rev.* B **36** 6520
[31] Fiorentini V, Methfessel M and Scheffler M 1993 *Phys. Rev.* B **47** 13 353
[32] Neugebauer J and Van de Walle C G 1994 *Phys. Rev.* B **50** 8067
[33] Wei A-H, Ferreira L G and Zunger A 1990 *Phys. Rev.* B **41** 8240
[34] Wright A F and Nelson J S 1994 *Phys. Rev.* B **50** 2159
[35] Korakakis D, Ludwig K F Jr and Moustakas T D 1997 *Appl. Phys. Lett.* **71** 72